表　　題　優性 WFS1 変異体の *in vitro* 機能解析とその機能レスキューに関する検討

(The functional analysis of dominant WFS1 pathogenic variants and its functional rescue)

論 文 の 区 分　博士課程

著者名　KHISHIGJARGAL BATJARGAL

担 当 指 導 教 員 氏 名　小児科学　・教授・山形 崇倫
研究指導協力教員　小児科学　・教授・田島 敏広

自治医科大学大学院医学研究科
専攻　地域医療学系
専攻分野　生殖・発達医学
専攻科　成育医学

２０２１年２月 25 日申請の学位論文

Table of Contents

Abstract

Wolfram syndrome (WS) is a rare disorder characterized by diabetes mellitus, optic atrophy, sensorineural deafness, diabetes insipidus, and neurodegeneration and that is caused by pathogenic variants in WFS1. WS is typically inherited as an autosomal recessive disorder, but autosomal dominant pathogenic variants have been identified. *WFS1* encodes a protein called wolframin, which is a transmembrane protein localized to the endoplasmic reticulum (ER). The localization of WFS1 indicates that it has physiological roles in the trafficking of membranes, secretion and regulation of ER calcium homeostasis. ER stress responses, including cell apoptosis, are caused because of the disruption or overloading of these functions.

We speculated these dominant WFS1 pathogenic variants were thought to increase ER stress. Recent studies suggest that 4-phenylbutyrate (PBA) and valproate (VPA) reduce ER stress. The objective of this study was to analyze the effect of PBA and VPA on dominant pathogenic WFS1 variants *in vitro.*

We determined whether dominant WFS1 variants (p.His313Tyr, p.Trp314Arg, p.Asp325_Ile328del, p.Glu809Lys, and p.Glu864Lys) increase ER stress and the dominant negative effect using by a luciferase assay of ER stress response element. In addition, the rescue of cell apoptosis induced by dominant WFS1 variants following treatment with PBA or VPA was determined by quantitative real-time PCR of C/EBP homologous protein (CHOP) mRNA expression. As results, these variants showed the increased ER stress and the dominant negative effect on the wild-type WFS1. After treatment with PBA or VPA, ER stress and cell apoptosis were reduced in each variant.

In conclusion, PBA and VPA could reduce the ER stress and cell apoptosis caused by dominant pathogenic WFS1 variants.

Key words: Wolfram syndrome, WFS1, Endoplasmic reticulum stress, 4-Phenylbutyrate, Valproate

1. Introduction

Wolfram syndrome (WS) is a rare genetic disorder showing child-onset diabetes mellitus (DM) caused by mutations in the gene encoding wolframin (*WFS1*) [1-3].

DM is the most prevalent metabolic condition in the world and has risen in incidence over the past decade. In 2011 the International Diabetes Federation reported that 366 million people had diabetes, with an estimated worldwide increase to 552 million by 2030 [4]. DM is a disorder in which the body does not produce sufficient insulin or fails to respond normally to the insulin produced, resulting in high levels of blood glucose [5]. Insulin is a hormone secreted by pancreatic β-cells that enhances glucose uptake and metabolism in the cells, thus reducing blood sugar level. In patients with DM, an insufficient secretion of insulin or a lack of response to insulin, resulting in high blood glucose level, is a status called hyperglycemia.

1.1 Major types of diabetes

Most cases of diabetes are classified into two major types: type 1 diabetes mellitus (T1DM) and type 2 diabetes mellitus (T2DM) [6]. T1DM progresses with an absolute deficiency of insulin due to the progressive autoimmune destruction of β-cells in the pancreas. It usually manifests in children and adolescents [7], and accounts for approximately 5–10% of all diabetic patients. T2DM is characterized by the body not responding effectively to insulin; this is termed insulin resistance [8]. It is caused by several factors, including insulin resistance, inadequate secretion of insulin, overweight and obesity. Patients with T2DM may affect diabetes-related complications, including cardiovascular disease, eye damage, kidney disease, nerve problems, skin infections, and diabetic foot disorders [9,10].

1.2 Monogenic diabetes

Some rare forms of DM result from one or more defects in a single gene, and are called monogenic. So far, more than 20 genetic subtypes have been detected in patients with

monogenic diabetes, accounting for approximately 1−6.5% of cases of diabetes in children [11-16]. The genetic form of DM is mostly classified into two types: neonatal diabetes mellitus (NDM) and maturity-onset diabetes of the young (MODY). According to their pathogenic mechanisms, it also can be classified as genetic defects of β-cell function and genetic defects of insulin action [17] (Table 1).

NDM typically appears before the age of six months [18], and is usually caused by a mutation in one of three genes: *KCNJ11, ABCC8, or INS.* Usually, MODY first appears in adolescence or early adulthood, is sometimes inherited as a dominant trait [19], and is more common than NDM. Defects in several genes, such as *hepatocyte nuclear factor (HNF) 4A, glucokinase, HNF1A,* and *HNF1B* are the causes of MODY (Table 1).

Table 1: Classification of genetic forms of DM

I.	Genetic defects of β-cell function	1. Neonatal diabetes • Transient (mutations in *PLAGL1/HYMAI, ZFP57, ABCC8, HNF1B)* • Permanent (mutations in *ABCC8, KCNJ11, INS, GCK, IPF1, FOXP3, EIF2AK3, GATA6*) 2. MODY 1-10: Mutations in *HNF4A, GCK, HNF1A, IPF1, HNF1B, NEUROD1, KLF1, CEL, PAX4, INS, BLK* 3. Mitochondrial DNA mutations (Pearson syndrome, Kearns−Sayre syndrome, and maternally inherited diabetes and deafness) 4. Wolfram syndrome • Wolfram syndrome 1 (WFS1) • Wolfram syndrome 2 (WFS2) 5. Thiamine responsive megaloblastic anemia and diabetes
II.	Genetic defects of insulin action	1. Type A insulin resistance 2. Donohue syndrome 3. Rabson-Mendenhall syndrome 4. Lipoatrophic diabetes syndrome

1.3 Wolfram syndrome

Wolfram syndrome (WS) is a rare genetic disorder caused by mutations in the gene encoding wolframin (*WFS1*) and is usually inherited as an autosomal recessive trait [1,20,21]. It manifests in childhood or early adulthood, is characterized by diabetes mellitus (DM), optic atrophy, sensorineural deafness, diabetes insipidus, and neurodegeneration [3,22], and is classified as child-onset monogenic diabetes. The estimated prevalence is 1 in 770,000 in the UK [23], 1 in 100,000 in North America [24], and 1 in 710,000 in the Japanese population [22].

Childhood-onset DM and progressive optic atrophy are the main diagnostic criteria for WS. DM is the first symptom of WS. It is usually diagnosed at around the age of six years, followed by optic atrophy at around the age of 11 [1]. Optic atrophy is characterized by loss of color and peripheral vision, and usually blindness within approximately eight years of the first signs of optic atrophy. Approximately 70% of patients with WS also develop central diabetes insipidus, and 65% of patients present sensorineural deafness in the second decade. More than 60% of WS patients experience neurological symptoms, most often presenting in early adulthood as difficulties with balance and coordination (ataxia) [2,3].

WS is usually inherited in an autosomal recessive manner. However, several dominant pathological variants in *WFS1* have been reported in patients with autosomal dominant adult-onset DM caused by the p.Trp314Arg variant [25], and in neonatal DM cases with congenital cataract and deafness caused by the p.Glu809Lys variant [26]. In addition, p.Asp325_Ile328del has been reported to cause neonatal early-onset severe WS [1], while p.His313Tyr was found in two unrelated patients with WS and with neonatal diabetes and deafness, respectively [27,28]. The p.Glu864Lys variant reportedly causes autosomal dominant optic atrophy associated with hearing impairment and low-frequency sensorineural hearing loss (LFSHL), which are classified under the name of Wolfram-like disorder (WS-like disorder) (OMIM #614296) [29-31]. The genetic variations in *WFS1* can lead to a spectrum of phenotypes, including susceptibility to T1DM, T2DM, WS, WS-like disorder, and LFSHL (Figure 1).

WFS1 encodes a protein called wolframin. Wolframin is a 100 KDa protein with nine transmembrane segments that localizes to the endoplasmic reticulum (ER) [3]. This protein is highly expressed in pancreatic β-cells, the brain, heart, retina, and inner ear cells [20,29,32]. In pancreatic β-cells, WFS1 plays an important role in proinsulin folding and processing in the ER [20,22]. So far, more than 120 pathogenic variants have been reported in *WFS1* from WS patients. These variants are mainly located at transmembrane domains, composed of a cytoplasm located N-terminal and an ER lumen located C-terminal [1,28].

WFS1 plays a key role in ER stress in β-cells, through negatively inhibiting transcription factor 6α (ATF6α). ATF6α is a main transcription factor involved in ER stress, with diminished ER stress response element (ERSE) promoter activation by ATF6α, and preserves E3 ubiquitin ligase-HRD1, thereby suppressing ER stress signaling. Conversely, chronic high basal unfolded protein response (UPR) levels are induced by WFS1 mutated pancreatic β-cells, and E3 ubiquitin ligase-HRD1 cannot be recruited to degrade activated ATF6 protein, leading to intolerable ER stress [33]. WFS1 has also been shown to be in dysregulation of calcium homeostasis [34], and misfolding of pathogenic forms of WFS1 induces ER stress in pancreatic β-cells, neurons, retinal ganglion cells, and oligodendrocytes, resulting in the dysfunction and degeneration of affected tissues [35].

An experimental model that generated β-cells *in vitro* by induction of pluripotent stem cells (iPSCs) derived from WS1 patients' skin cells were developed by Shang et al [36]. This study showed that iPSCs had high levels of ER stress and decreased insulin content [36]. In addition, mitochondrial dynamics can also change ER dysfunction, leading to the neuropsychiatric aspects of this disorder [37].

Currently, there is no effective treatment for WS. DM of patients with WS is treated with insulin supplementation, but control of DM is difficult, and neural complications cannot be treated. The main neurologic complications in WS include cerebellar ataxia, peripheral

neuropathy, and cognitive impairment. The prognosis of this disease is poor; the median age of death is 30 years (25–49) due to central apnea with brain stem atrophy [38]. Thus, understanding the molecular mechanism of pancreatic and neuronal cell death in WS may aid the search for treatments for this disease.

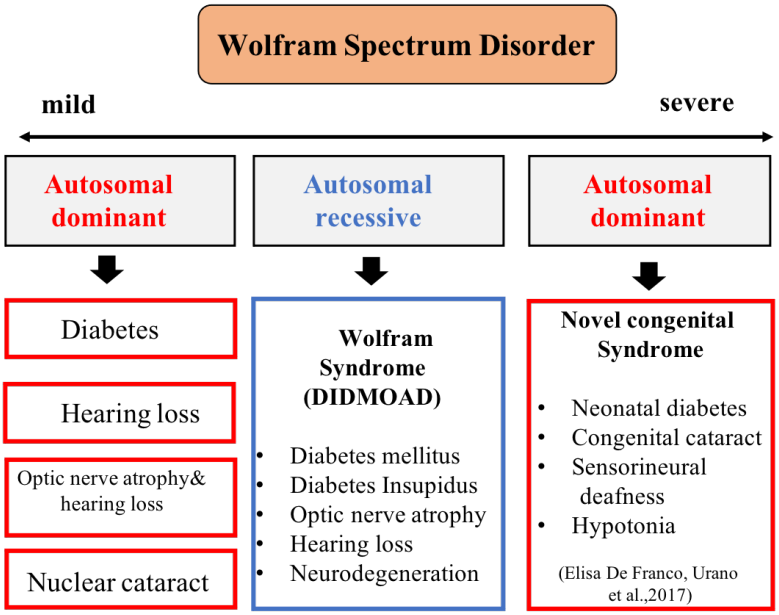

Figure 1. Clinical symptoms caused by autosomal dominant and autosomal recessive *WFS1* variants.

1.4 ER homeostasis

The ER is an important organelle in the cells. It plays a key role in protein transport and synthesis, protein folding, lipid and steroid synthesis, and calcium storage [39]. Two functionally distinct types can be categorized into the ER: the smooth endoplasmic reticulum (SER) and the rough endoplasmic reticulum (RER). The ER is the major location of protein modification, which has a crucial function in the protein folding process for secretory proteins such as insulin, cell surface receptors, and integral membrane proteins [40].

When problems occur in protein synthesis and folding, the RER is able to send signals immediately to the nucleus and thus affect the overall rate of protein translation. A multitude of pathological and physiological factors impair ER function and cause

ER homeostasis dysregulation, resulting in ER stress.

The unfolded protein response (UPR) is triggered when excessive misfolded or unfold ed proteins accumulate in the ER [41]. The UPR works to remove the level of misfolded proteins as a pro-survival response and to restore ER function [8]. However, apoptosis is activated in cases where ER stress becomes prolonged or persistent for UPR-based mitigation [42] (Figure 2).

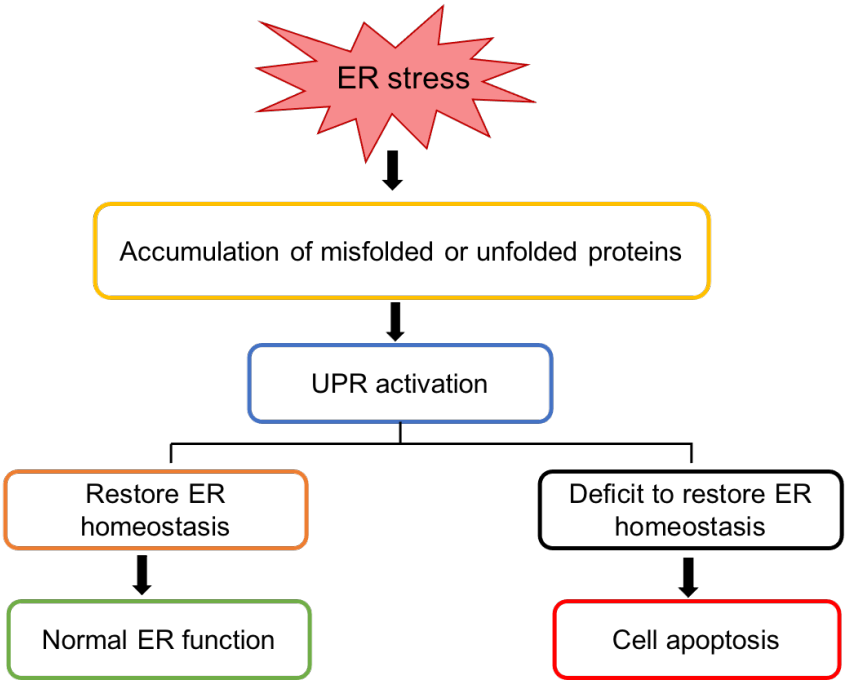

Figure 2. The role of the unfolded protein response (UPR) against ER stress. UPR is a pro-survival response designed to relieve misfolded protein accumulation, restore ER homeostasis, and restore normal function of ER. However, cell apoptosis is caused if the UPR signaling system fails to restore ER homeostasis.

1.4.1 UPR signaling system

The unfolded or misfolded proteins interconnect with ER localized chaperone-immunoglobulin binding protein (BiP) when ER stress occurs in the cells, removing it from ER stress sensors, therefore activating downstream signaling pathways. The UPR signaling

system is regulated by three major sensors: protein kinase-like ER kinase (PERK), ATF6, and inositol-requiring enzyme 1 (IRE1) (Figure 3).

PERK is an ER transmembrane protein kinase of the PEK family that is found in the ER lumen and binds to BiP. When ER stress occurs, PERK releases BiP and activates the phosphorylation of eukaryotic translation initiation factor 2 alpha (eIF2α), leading to reduction of general protein synthesis. This translational control offers an effective means of reducing the protein load in the ER. At the same time, ATF4 is activated by PERK-phosphorylated eIF2α, which translocates to the nucleus and activates the transcription of genes needed to restore ER homeostasis [42].

ATF6 is another transcription factor that can sense ER stress. ATF6 preserves its resting form in the ER under normal conditions and is associated with BiP. In response to ER stress, ATF6 is sequestered away from BiP and moves from the ER to the Golgi apparatus, where site-1 protease (S1P) and site-2 protease (S2P) cleave into its active type. A soluble basic leucine zipper (bZip) transcription factor generates this cleavage of ATF6, which transits to the nucleus. In the nucleus, ATF6 induces transcriptional activation of ER stress-response genes along with ER stress-response elements 1 and 2 (ERSE-1 and 2).

IRE1 is an ER transmembrane glycoprotein comprising the domain of serine-threonine kinase and an endoribonuclease activity [43]. IRE1 interacts with BiP under unstressed conditions and maintains an inactive form. IRE1 is sequestered away from BiP and changes to its active form when ER stress occurs. The endonuclease activity of IRE1, which is activated by its dimerization and transphosphorylation, processes unspliced X box-binding protein 1 (XBP1u) encoding mRNA to generate an active transcription factor, spliced XBP1 (XBP1s) [44]. Including genes involved in protein folding and the ER associated degradation (ERAD) process, XBP1s regulates downstream UPR signaling. IRE1 will activate pro-apoptotic signal

cascades, such as the c-Jun N-terminal kinase (JNK) signaling pathway, if ER stress is permanent [33].

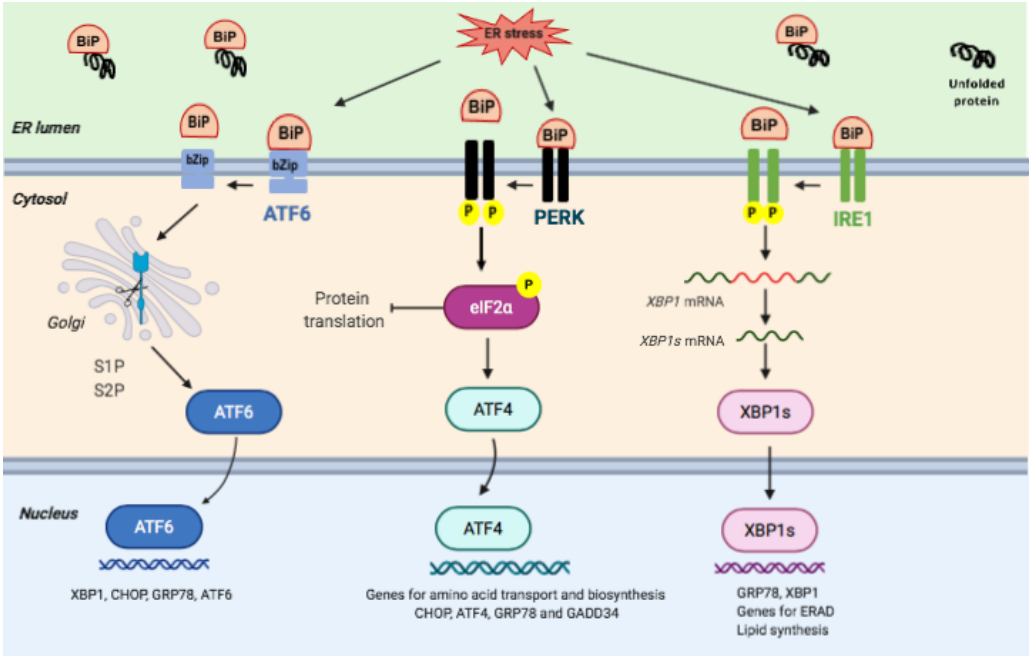

Figure 3. The UPR signaling pathway. UPR is regulated by three major sensors (PERK, ATF6, and IRE1). The ER molecular chaperone, BiP, interacts directly with these UPR sensors under normal circumstances. Under abnormal conditions in the ER, PERK releases BiP and induces phosphorylation of eIF2α that can prevent the initiation of translation and reduce the general protein synthesis. ATF4 is also induced by PERK-phosphorylated eIF2, which transits to the nucleus and activates the transcription genes required to restore ER homeostasis. When BiP is isolated from ATF6, ATF6 is translocated from the ER to Golgi, where it is cleaved into its active form by S1P and S2P. A soluble basic leucine zipper (bZip) transcription factor is produced by this cleavage of ATF6, which migrates to the nucleus and induces transcriptional activation of ER stress-response genes along with ERSE-1 and 2. In addition, IRE1 is activated through its dimerization and transphosphorylation and processes the mRNA encoding XBP1u to produce XBP1s. This spliced form of XBP1 transits to the nucleus and regulates downstream UPR signaling, including genes involved in ERSE and ERAD. The UPR sensors induce the pro-apoptotic pathways, leading to cell apoptosis under permanent ER stress conditions. The figure was created by Biorender software.

1.4.2 ER stress-related diseases

Chronic or severe and persistent ER stress triggers the leading UPR cell death involved in a number of diseases, including metabolic disease, neurodegenerative disease, inflammatory disease, and cancer. ER stress plays a key role in failure of β-cells, both in humans and in rodent models [45]. In T1DM, β-cell failure is induced by excessive nitric oxide (NO) production; it depletes ER Ca^{2+}, induces ER stress, and leads to apoptosis [46]. Increased CHOP, BiP, *Xbp1* mRNA splicing, and increased eIF2α phosphorylation levels have been identified in *db/db* mice islets, a common model of insulin resistance and β-cell failure [47,48]. Signs of ER stress were observed in islets, liver, and adipose tissue in T2D mouse models [47], and the classical UPR-induced proteins $p58^{IPK}$, BiP, and CHOP were significantly elevated in pancreatic islet tissue in patients with T2D patients [49].

The pancreatic β-cells with *WFS1* pathogenic variants have chronic high basal UPR levels, as reported by Fonseca et al. [33]. Thus, E3 ubiquitin ligase-HRD1 cannot be recruited to degrade activated ATF6 protein, leading to intolerable ER stress. *Wfs1* knocked out mice and also showed high UPR marker expression and defective insulin production [50,51].

Wolcott–Rallison syndrome (WRS), an autosomal recessive rare disease with permanent neonatal or early infancy insulin-dependent diabetes, mental retardation, and developmental delay, is another typical ER stress disease. Patients with WRS have pathogenic variants in the eukaryotic translation initiation factor 2-α kinase 3 (*EIF2AK3*) gene, which encodes the PERK protein [52]. Therefore, UPR signaling components are emerging as potential targets for human disease intervention and treatment.

1.5 4-phenylbutyrate and valproate

4-phenylbutyrate (PBA) is a low molecular weight fatty acid and chemical chaperone [53]. It has been shown to prevent the mis-localization and/or aggregation of proteins associated

with human disease [54,55]. PBA reportedly alleviates ER stress by decreasing the protein folding load [54,56,57]. Moreover, PBA has been shown to restore normal insulin synthesis and to have the ability to upregulate insulin secretion in the stem cell model of WS [32,36]. In addition, PBA reduces ER stress in pancreatic β-cells induced by high glucose *in vitro* and *in vivo* [58].

Valproate (VPA) is a simple branched-chain fatty acid that has been used widely as an anti-convulsant and mood-stabilizing drug [59]. While its exact mechanism of action has yet to be determined, several studies have reported that VPA attenuates ER stress-induced apoptosis in neuronal and hepatocellular cells [60,61] and protects pancreatic β-cells from palmitate-induced ER stress and cell apoptosis [62]. In addition, acute VPA treatment has been shown to improve glucose tolerance in *Wfs1* mutant mice with elevated ER stress response [63].

1.6 Purpose of our study

Despite the underlying significance of ER dysfunction in WS, molecular mechanisms linking the ER to β-cell death have not yet been clarified. The purpose of our study is to elucidate the molecular mechanism of pancreatic β-cell death by dominant WFS1 pathogenic variants *in vitro*. In addition, we analyze the effects of PBA and VPA on dominant pathological variants.

2 Materials and Methods

2.1 Cell culture

Human embryonic kidney (HEK)-293 cells were cultured in DMEM (Invitrogen, Carlsbad, CA) with 10% heat-inactivated fetal bovine serum and 1% penicillin/streptomycin. MIN6 cells, which was established from an insulinoma of a transgenic mouse expressing the SV40 T antigen in pancreatic β-cells were cultured in DMEM (Invitrogen, Carlsbad, CA) with 15% heat-inactivated fetal bovine serum, 1% penicillin/streptomycin and 220 nM 2-mercaptoethanol. HeLa cells were cultured in MEM (Sigma-Aldrich, St. Louis, MO) with 10% fetal bovine serum at 37 °C in a humidified atmosphere of 5% CO2.

2.2 Site-directed mutagenesis and plasmid construction

We selected p.His313Tyr, p.Trp314Arg, p.Asp325_Ile328del, p.Glu809Lys, and p.Glu864Lys, (Figure 4) as dominant variants of WFS1 [1,20,21] and p.Pro724Leu and p.Arg629Trp [20,22] as recessive variants. The membrane topology of WFS1 was analyzed with TMHMM (http://www.cbs.dtu.dk/services/TMHMM/). Human wild-type WFS1 cDNA was inserted into a pcDNA3.1 expression vector [1]. The plasmids that contain WFS1 pathological variant were (p.His313Tyr, p.Trp314Arg p.Glu809Lys, p.Glu864Lys, p.Pro724Leu and p.Arg629Trp) created by site-directed mutagenesis using a Gene-Art Mutagenesis Kit (Invitrogen, Carlsbad, CA). In addition, a wild-type WFS1 plasmid tagged with green fluorescent protein (GFP) at the N-terminus, which was generated from WFS1 cDNA fragments and the pGFP-vector (Clontech Laboratories, Mountain View, CA), was also mutagenized. These five GFP-tagged dominant WFS1 variants were confirmed by DNA sequencing before transfection. For mutagenesis, the following sets of primers were used for plasmid construction (Table 2).

Table 2. Primer sequence for mutagenesis contain WFS1 pathogenic variants

	WFS1 pathogenic variants	Primer sequence
1.	p.His313Tyr (c.937C>T)	Forward 5' TCCAGGGCAGGCATGTACTGGCTGTCCACCA 3'
		Reverse 5' TGGTGGACAGCCAGTACATGCCTGCCCTGGA 3'
2.	p.Trp314Arg (c.940T>C)	Forward 5' AGGGCAGGCATGCACAGGCTGTCCACCATCA 3'
		Reverse 5' TGATGGTGGACAGCCTGTGCATGCCTGCCCT 3'
3.	p.Glu809Lys (c.2425G>A)	Forward 5' CTGCGGGCCAGCAGCAAGTTCAAGAGCGTGC 3'
		Reverse 5' GCACGCTCTTGAACTTGCTGCTGGCCCGCAG 3'
4.	p.Glu864Lys (c.2590G>A)	Forward 5' CGGCACGTGAAGATCAAGCACGACTGGCGCA 3'
		Reverse 5' TGCGCCAGTCGTGCTTGATCTTCACGTGCCG 3'
5.	p.Pro724Leu (c.2171C>T)	Forward 5' CCATCAACATGCTCCTGTTCTTCATCGGCGA 3'
		Reverse 5' TCGCCGATGAAGAACAGGAGCATGTTGATGG 3'
6.	p.Arg629Trp (c.1885C>T)	Forward 5' GTGAAGTCCCTGACGTGGAGCTCCATGGTCA 3'
		Reverse 5' TGACCATGGAGCTCCACGTCAGGGACTTCAC 3'

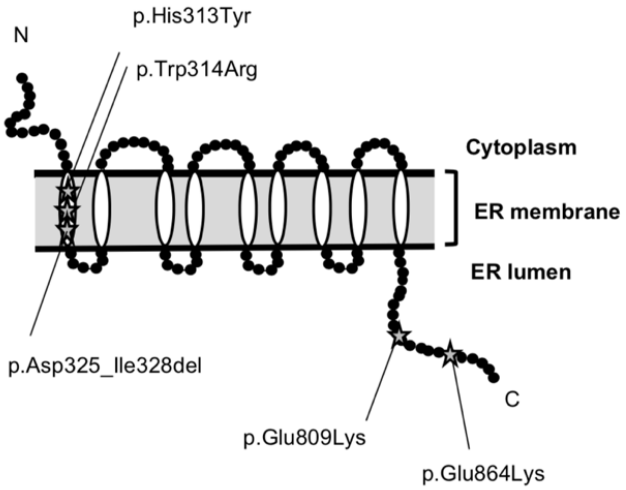

Figure 4. The positions of the dominant variants we constructed are represented as asterisks.

2.3 Luciferase reporter assay

2.3.1 Endoplasmic reticulum stress response element (ERSE)-luciferase assay

For reporter assays, HEK-293 and MIN6 in a 24-well plate were transfected with 1.0 μg of each wild-type or pathological WFS1 variant (p.His313Tyr, p.Trp314Arg, p.Asp325_Ile328del,

p.Glu809Lys, p.Glu864Lys, p.Pro724Leu and p.Arg629Trp) expression plasmid together with 0.5 μg ERSE luciferase plasmid [1] and 10.0 ng Renilla reniformis luciferase plasmid. Cell lysates were harvested and assayed for Renilla and firefly luciferase activity using the Dual Luciferase Reporter Assay System at 28 h or 48 h after transfection (Promega, Madison, WI). ERSE-luciferase activity was normalized to Renilla reniformis luciferase activity. All reactions were performed in triplicate and the experiments were repeated 3 times.

2.3.2 Activating transcription factor 6 α (ATF6α)-luciferase reporter assay

HEK-293 and MIN6 cells in a 24-well plate were transfected with 1.5 μg of each wild-type or WFS1 variant expression plasmid together with 0.5 μg pGL4.39 (luc2P/ATF6) and 0.5 μg ATF6α expression plasmid and 10.0 ng Renilla reniformis luciferase plasmid [1]. A luciferase reporter vector [pGL4.39 (luc2P/ATF6)] containing an ATF6 response element that drives transcription of the luciferase reporter gene luc2P (Photinus pyralis). At 28 h or 48 h after transfection, cell lysates were harvested and assayed for Renilla and firefly luciferase activity using the Dual Luciferase Reporter Assay System (Promega, Madison, WI). ERSE-luciferase activity was normalized to Renilla reniformis luciferase activity. All reactions were performed in triplicate and the experiments were repeated 3 times.

2.3.3 Effect of PBA and VPA on ER stress

To analyze the effect of PBA and VPA on ERSE activity, HEK-293 and MIN6 in a 24-well plate were transfected with 1.0 μg of wild-type or each WFS1 pathological variant (p.His313Tyr, p.Trp314Arg, p.Asp325_Ile328del, p.Glu809Lys, p.Glu864Lys, p.Pro724Leu and p.Arg629Trp) expression plasmid together with 0.5 μg ERSE luciferase plasmid [1] and 10.0 ng Renilla reniformis luciferase plasmid. At 24 h after transfection, the growth medium was replaced with fresh medium containing 4 mM PBA or 6 mM VPA (both from Sigma-

Aldrich, St. Louis, MO) [1,58,62] for 24 h. After treated with PBA or VPA, cell lysates were harvested and assayed for Renilla and firefly luciferase activity using the Dual Luciferase Reporter Assay System (Promega, Madison, WI). ERSE-luciferase activity was normalized to Renilla reniformis luciferase activity. All reactions were performed in triplicate and the experiments were repeated 3 times.

2.4 Quantitative real-time PCR analysis

HEK-293 cells and MIN6 cells were plated on a 3-cm dish and cultured to 70–80% confluency. The cells were transfected with 5.0 μg of each wild-type or each WFS1 pathological variant expression plasmid. After transfection for 24 h, total mRNA was isolated from the cells using a RNeasy Mini Kit (QIAGEN, Hilden, Germany). The reverse transcription products were amplified using a SYBR Premix Ex TaqTM II Kit (Takara, Shiga, Japan) on an Applied Biosystems® 7500 Fast Real-Time PCR System (Applied Biosystems, Life Technologies, Carlsbad, CA) and the following program: 95 °C for 30 s followed by 40 cycles at 95 °C for 3 s and 60 °C for 30 s. Values are presented as the mean ± standard deviation (SD) and normalized to the amount of GAPDH. We performed the same experiment with MIN6 cells for dominant variants of p.His313Tyr, p.Asp325_Ile328del, p.Glu809Lys. For qPCR, the following sets of primers and SYBR Green PCR master Mix (Takara, Shiga, Japan) were used for real-time PCR: human C/EBP homologous protein (CHOP) (forward) 5′-AGAACCAGGAAACGGAAACAGA-3′ and (reverse) 5′-TCTCCTTCATGCGCTGCTTT-3′ and GAPDH (forward) 5′-CTTTGTCAAGCTCATTTCCTGG-3′ and (reverse) 5′-TCTTCCTCTTGTGCTCTTGC-3′. All reactions were performed in triplicate and the experiments were repeated 3 times.

2.4.1 Effect of PBA and VPA on cell apoptosis

HEK-293 cells and MIN6 cells were plated on a 3-cm dish and cultured to 70–80% confluency. The cells were transfected with 5.0 μg of wild-type or each WFS1 pathogenic expression plasmid. To determine the effect of PBA and VPA on CHOP mRNA, at 4 h after transfection, the growth medium was replaced with fresh medium containing 0.5 mM PBA [54] or 0.25 mM VPA [60,62,64] for 16 h. After treated with PBA or VPA, total mRNA was isolated from the cells using a RNeasy Mini Kit (QIAGEN, Hilden, Germany). The reverse transcription products were amplified using a SYBR Premix Ex TaqTM II Kit (Takara, Shiga, Japan) on an Applied Biosystems® 7500 Fast Real-Time PCR System (Applied Biosystems, Life Technologies, Carlsbad, CA) and the following program: 95 °C for 30 s followed by 40 cycles at 95 °C for 3 s and 60 °C for 30 s. All reactions were performed in triplicate and the experiments were repeated 3 times. Values are presented as the mean ± standard deviation (SD) and normalized to the amount of GAPDH.

2.5 Western blot analysis

HEK-293 cells were plated on a 3.5-cm dish and cultured to 70–80% confluency. The cells were transfected with 5.0 μg GFP-tagged wild-type or each dominant WFS1 variant expression plasmid. At 24 hr transfection, the transfection efficiency of each vector was evaluated by number of GFP-positive cells/total number of cells per field using fluorescence microscopy. The cells were lysed with ice-cold TNE buffer containing 20 mM Tris-HCl, 0.5% Triton X-100, 1 mM EDTA (pH 7.4) for 5 min on ice. The lysates were centrifuged at 15,000 x g for 30 min at 4°C. After centrifugation, protein concentration was determined using a Qubit Protein Assay Kit (Invitrogen, Carlsbad, CA). Protein lysates were normalized to total protein (25 μg/lane) and resolved by 5–12.5% gradient sodium dodecyl sulfate-polyacrylamide gel electrophoresis followed by electro-transfer of the proteins onto a polyvinylidene fluoride

membrane. The membrane was blocked with 5% skimmed milk/phosphate-buffered saline with Tween 20 (PBST) for 1 h at room temperature. The membrane was incubated with the following primary antibodies: anti-GFP (1:200; SC-9996; Santa Cruz Biotechnology, Santa Cruz, CA) and mouse monoclonal anti-β-actin (1:5000; A1978; Sigma-Aldrich, St. Louis, MO) in PBST overnight at 4 °C. After washing 3 times with PBST for 10 min, anti-mouse IgG HRP (1:2000; SC-516102; Santa Cruz Biotechnology, Santa Cruz, CA) was used as a secondary antibody for 1 h at room temperature. After washing 3 times with PBST for 15 min, the membrane was detected with HRP Substrate (Takara, Shiga, Japan) and imaged using Image Quant LAS 4000 (GE Healthcare, Little Chalfont, UK). Hyper HRP substrate was purchased from TAKARA (Shiga, Japan).

2.6 Fluorescence analysis and confocal microscopy

HeLa cells were plated on an 8-well chamber slide and transfected with 1.0 μg GFP-tagged wild-type or each dominant WFS1 expression plasmid. At 24 h after transfection, the ER was stained using an ER-ID Red Assay Kit (Enzo Life Science, New York, NY) according to the manufacturer's protocol. The cells were fixed in 4% paraformaldehyde/PBS for 15 min at room temperature. The stained ER and GFP fluorescence were examined by confocal microscopy (FLUOVIEW FV1000; Olympus, Tokyo, Japan).

2.7 The effect of PBA and VPA on the protein localization

2.7.1 Assay by confocal microscopy

HeLa cells were plated on an 8-well chamber slide and transfected with 1.0 μg GFP-tagged wild-type or each dominant WFS1 variant (p.His313Tyr, p.Asp325_Ile328del, p.Glu809Lys) expression plasmid. At 24 h after transfection, cells were treated with or without 0.5mM PBA and 0.25 mM VPA for 16 hr. After treated with PBA or VPA, the ER was stained using an ER-ID Red Assay Kit (Enzo Life Science, New York, NY) and the nuclei were stained blue

(Hoechst 33342). The cells were fixed in 4% paraformaldehyde/PBS for 15 min at room temperature. The stained ER and GFP fluorescence were examined by confocal microscopy (FLUOVIEW FV1000; Olympus, Tokyo, Japan).

2.7.2 Assay by IN cell analyzer

HeLa cells in 96-well plate were transfected with 0.1 μg GFP-tagged wild-type or each dominant WFS1 variant. At 24 h after transfection, cells were treated with or without 0.5mM PBA and 0.25 mM VPA for 16 hr, and the intensity of the fluorescence were measured by IN cell analyzer 1000 (GE healthcare).

Statistical analysis

All data are represented as the mean ± (SD). Multiple comparisons between groups were carried out with one-way ANOVA (or Kruskal Wallis test). *Post hos* analysis was performed by Tukey's test except for p.Asp325_Ile328del, which was tested by non-parametric analysis, because of non-normal distribution. Two tailed Student's *t*-test was used for comparisons between untreated or treated groups using PBA and VPA. All data were analyzed by GraphPad Prizm version 8.0 (GraphPad Software Inc., San Diego, CA, USA). $P < 0.05$ was considered significant in all analysis. In the figures, the numbers below the lanes of blots denote relative protein amounts, as quantified by ImageJ software, normalized to the respective control.

3 Results

3.1 Luciferase reporter assay

3.1.1 ERSE-luciferase assay

All of the dominant WFS1 variants activated ERSE reporter activity significantly more than wild-type WFS1, however recessive variants did not statistically increase ERSE reporter activity (Figure 5a). The results for p.His313Tyr, p.Trp314Arg, p.Asp325_Ile328del, p.Glu809Lys and p.Pro724Leu were in agreement with previous reports [1,25,26,28]. Regarding p.Glu864Lys, its functional consequence has not been determined previously; however, we found that this variant also increased ER stress. The degree of ER stress was highest for the p.Asp325_Ile328del variant compared to the other variants (Figure 5a). Moreover, when cells were equally co-transfected with wild-type, dominant or recessive WFS1 expression plasmid, ER stress was still elevated by all dominant variants but not recessive variants (Figure 5b).

These results indicated that each dominant WFS1 variant has a dominant negative effect on the wild type, but recessive variants do not have a dominant negative effect (Figure 6b). When MIN6 cells were used in ERSE-luciferase reporter assay, p.His313Tyr, p.Glu809Leu and p.Asp325_Ile328del significantly increased the reporter activity, but p.Trp314Arg and p.Glu864Lys did not increase (Figure 6).

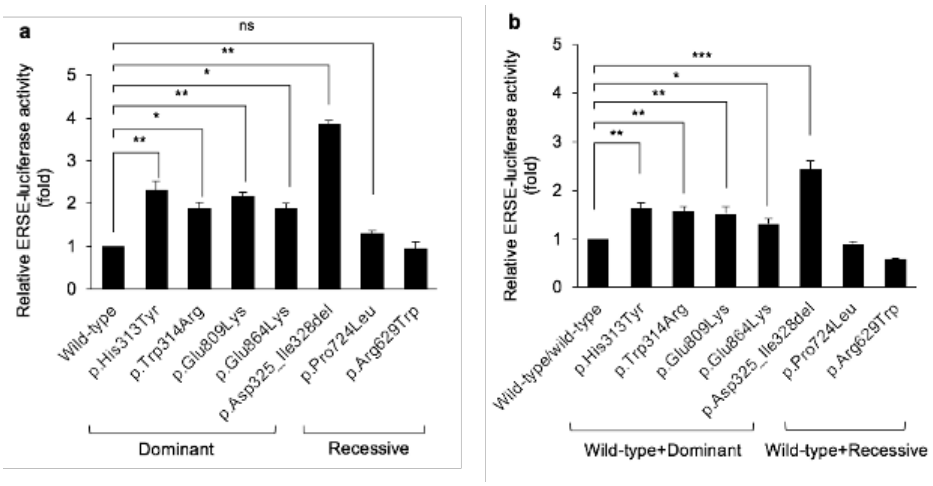

Figure 5. Luciferase reporter assays in HEK-293 cells. a, Cells were transfected with the ERSE reporter vector and the wild-type or dominant (p.His313Tyr, p.Trp314Arg, p.Asp325_Ile328del, p.Glu809Lys, p.Glu864Lys) or recessive WFS1 pathogenic variant (p.Pro724Leu and p.Arg629Trp) expression plasmid. All of the dominant WFS1 variants activated ERSE reporter activity significantly more than wild-type WFS1, however recessive variants did not statistically increase ERSE reporter activity. **b,** Cells were transfected ERSE reporter vector simultaneously in wild-type WFS1 alone or wild-type together with dominant or recessive WFS1 variants to elucidate the dominant negative effect. Each dominant WFS1 pathogenic variant exerted a dominant negative effect on the wild type, but recessive variants did not.

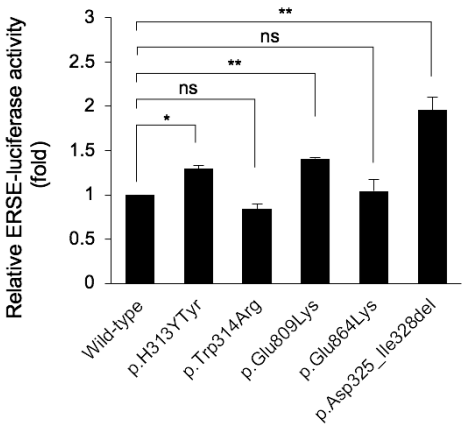

Figure 6. ERSE-luciferase reporter assay in MIN6 cells. Cells were transfected with the ERSE reporter vector and the wild-type or dominant pathogenic (p.His313Tyr, p.Trp314Arg, p.Asp325_Ile328del, p.Glu809Lys, p.Glu864Lys) WFS1 expression plasmid. p.His313Tyr, p.Glu809Leu and p.Asp325_Ile328del significantly increased the reporter activity, but p.Trp314Arg and p.Glu864Lys did not increase. Values are represented as the mean ± SD. Significant differences are indicated with *$p < 0.05$; **$p < 0.01$; ns nonsignificant.

3.1.2 ATF6α-luciferase reporter assay

At first, we examined whether the ATF6α promoter activity increases without ATF6α expression vector in HEK-293 cells. As shown, the ATF6α promoter activity did not increase without ATF6α expression vector (Figure 7). When HEK-293 cells were used, all dominant WFS1 pathogenic variants activated ATF6α promoter activity significantly more than wild-type WFS1, but recessive variants did not activate ATF6α promoter activity (Figure 8a). We performed the same experiment using MIN6. Results were the same as the experiment using ERSE-luciferase assay (Figure 8b).

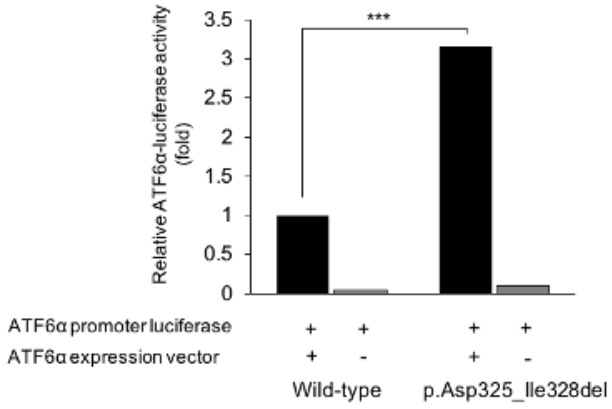

Figure 7. ATF6α-luciferase reporter assay in HEK-293 cells. Cells were transfected pGL(luc2P/ATF6) reporter vector and the WFS1 plasmid (wild-type or p.Asp325_Ile328del) with or without ATF6α expression vector. ATF6 promoter activity did not increase without ATF6α expression vector

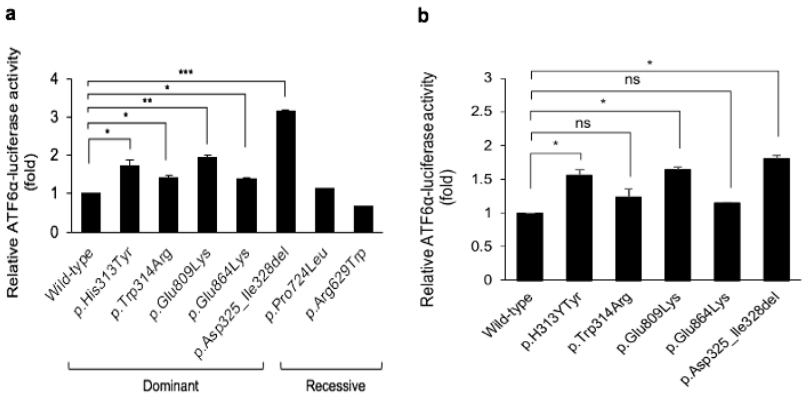

Figure 8 a, ATF6α-luciferase reporter assay in HEK-293 cells. Cells were transfected with the pGL4.39 (luc2P/ATF6) vector and ATF6α expression plasmid together with the wild-type or dominant or recessive WFS1 expression plasmid. All dominant WFS1 variants activated ATF6α promoter activity significantly more than wild-type WFS1, but recessive variants did not. **b, ATF6α-luciferase reporter assay in MIN6 cells.** p.His313Tyr, p.Glu809Leu and p.Asp325_Ile328del significantly increased the reporter activity, but p.Trp314Arg and p.Glu864Lys did not statistically increase. Values are represented as the mean ± SD. Significant differences are indicated with *$p < 0.05$, ns nonsignificant.

3.2. Expression of CHOP mRNA

Quantitative real-time PCR showed that all dominant WFS1 pathogenic variants induced a significant increase of CHOP mRNA in HEK-293 cells (Figure 9a). Also in MIN6, p.His313Tyr, p.Asp325_Ile328del, and p.Glu809Lys showed a significant increase of CHOP mRNA (Figure 9b). These findings suggest increased cell apoptosis by elevated ER stress.

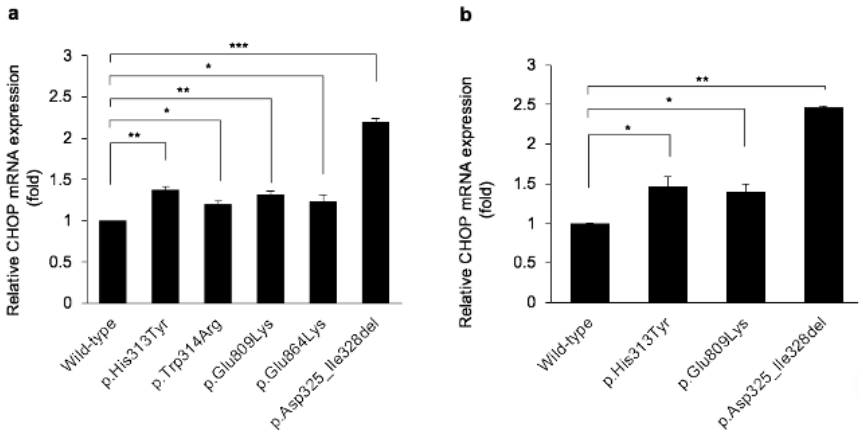

Figure 9 Quantitative PCR analysis of CHOP mRNA. a, HEK293 cells were transfected with the wild-type or pathological variant of WFS1 (p.His313Tyr, p.Trp314Arg, p.Asp325_Ile328del, p.Glu809Lys, and p.Glu864Lys) expression plasmid. After transfection for 24 h, mRNA was extracted from the cells and RT-PCR was performed followed by quantitative PCR. **b,** MIN6 cells were transfected with the wild-type or each WFS1 variant (p.His313Tyr, p.Glu809Lys and p.Asp325_Ile328del) expression plasmid. After transfection for 24 h, mRNA was extracted from the cells and RT-PCR was performed followed by quantitative PCR reactions were performed in triplicate and the experiment was repeated 3 times. Values are represented as the mean ± SD. Significant differences are indicated with *$p < 0.05$; **$p<0.01$; ***$p<0.001$.

3.3 Protein expression of dominant WFS1 pathogenic variants

We examined the expression levels of WFS1 protein by western blot analysis of each variant. When HEK-293 cells were used, approximately 60% of the transfection efficiency for all variants was observed, not different for each variant. As shown in Figure 10, the expression levels of p.His313Tyr, p.Asp325_Ile328del, p.Glu809Lys, and p.Glu864Lys were lower than that of wild-type WFS1, consistent with previous reports [1,26]. The p.Trp314Arg variant was expressed at a higher level than wild-type WFS1. The expression levels of p.Trp314Arg in fibroblasts from two patients with this variant were equivalent or slightly increased compare to that of control fibroblasts [25]. The increased expression level of p.Trp314Arg *in vitro* were consistent with the report.

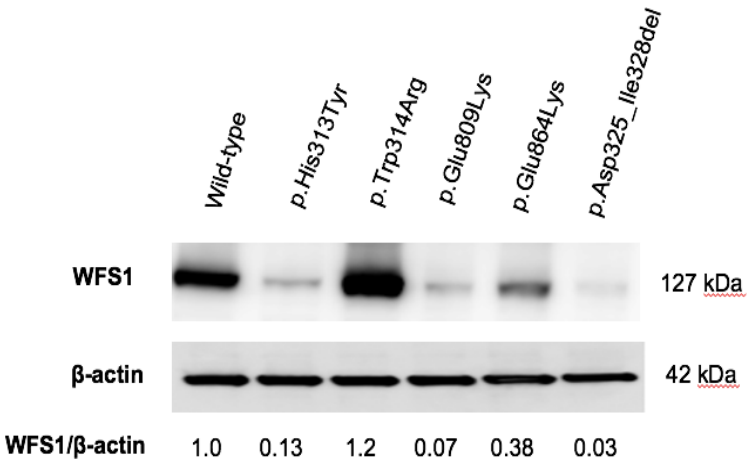

Figure 10. Western blot analysis of WFS1 protein. HEK-293 cells were transfected with the GFP-tagged wild-type or WFS1 pathogenic variant (p.His313Tyr, p.Trp314Arg, p.Asp325_Ile328del, p.Glu809Lys, and p.Glu864Lys) expression plasmid. Relative densitometry measurements (WFS1/β-actin) were calculated using ImageJ software.

3.4. Intracellular localization of WFS1 pathogenic variants

A diffuse reticular pattern that colocalized with the ER in HeLa cells was shown by GFP-tagged wild-type WFS1 (Figure 11). In contrast, all dominant WFS1 variants showed a punctate

staining pattern in the ER. These findings suggested that these dominant WFS1 variants may be misfolded and aggregate in the ER, in agreement with a previous study [26]. Among them, p.Glu809Lys and p.His313Tyr generated a highly punctate staining pattern in the ER.

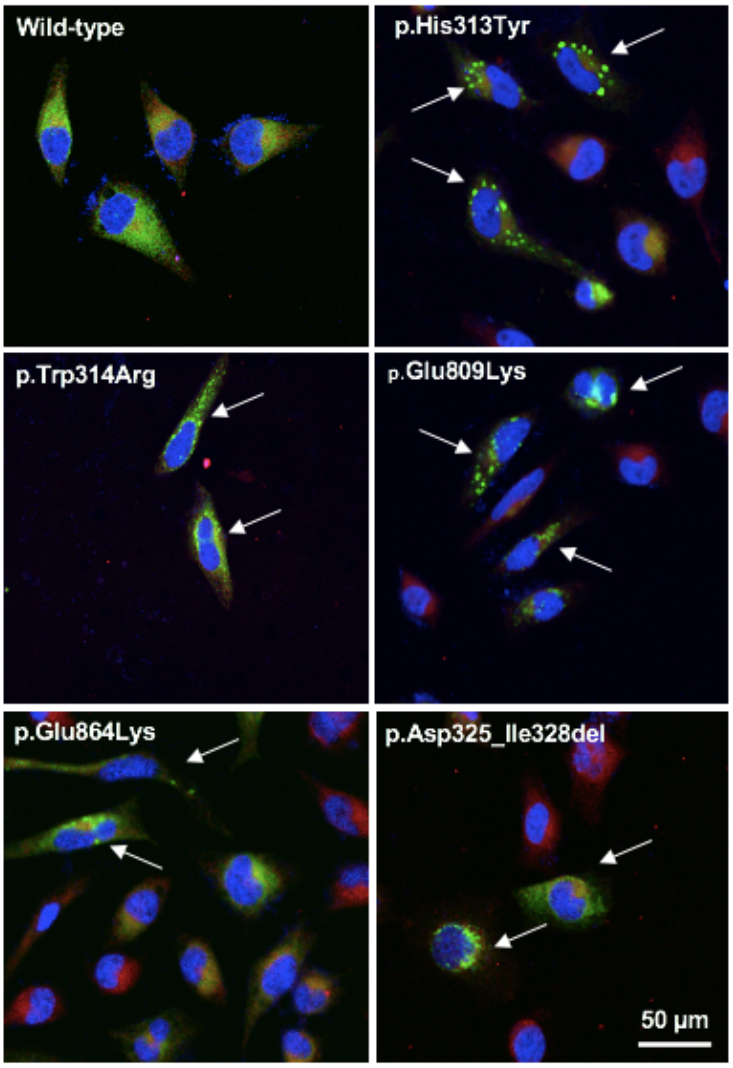

Figure 11. Double immunofluorescence of wild-type and WFS1 pathogenic variant pathological. HeLa cells were transiently transfected with the GFP-tagged wild-type or dominant WFS1 variant (p.His313Tyr, p.Trp314Arg, p.Asp325_Ile328del, p.Glu809Lys, and p.Glu864Lys) expression plasmid. The location of the ER was detected using an ER-ID Red Assay Kit. Scale bar 50μm. The nuclei were stained blue (Hoechst 33342). All dominant WFS1 variants showed a punctate staining pattern in the ER (white arrows); especially p.Glu809Lys and p.His313Tyr showed a highly punctate staining pattern in the ER. Each image was taken using a confocal microscopy.

3.6. Effect of PBA

We determined the effect of PBA on ERSE-luciferase activity and the expression level of CHOP mRNA. In MIN6 cells, ER stress and expression levels of CHOP mRNA of p.His313Tyr, p.Asp325_Ile328del, and p.Glu809Lys were significantly reduced by PBA (Figure 12a, b). In HEK-293 cells, ER stress were also reduced by PBA in all variants (Figure 13a). The expression levels of CHOP mRNA were significantly reduced by PBA for the p.His313Tyr, p.Asp325_Ile328del, p.Glu809Lys, and p.Glu864Lys variants in HEK-293 cells. For p.Trp314Arg, PBA treatment tended to reduce the expression of CHOP mRNA compared with wild-type WFS1 (Figure 13b).

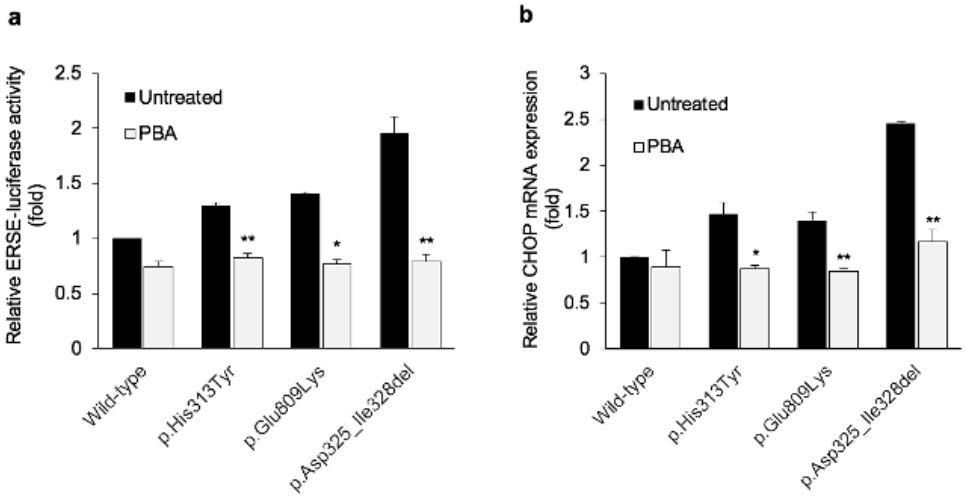

Figure 12. Effect of PBA in MIN6. a, Analysis of ERSE luciferase activity. MIN6 cells were transfected with the ERSE reporter vector together with the wild-type or WFS1 pathogenic variant (p. His313Tyr, p. Glu809Lys and p.Asp325_Ile328del) expression plasmid. Transfected MIN6 cells were treated with 4 mM PBA for 24 h. ERSE activity was normalized to activity with *Renilla reniformis* luciferase **b,** Quantitative PCR analysis of CHOP mRNA. After 4 h transfection, MIN6 cells were treated with 0.5 mM PBA for 16 h. mRNA was extracted from the cells and RT-PCR was performed followed by quantitative PCR. CHOP mRNA levels were normalized by GAPDH. Significant differences are indicated with *$p < 0.05$; **$p < 0.01$.

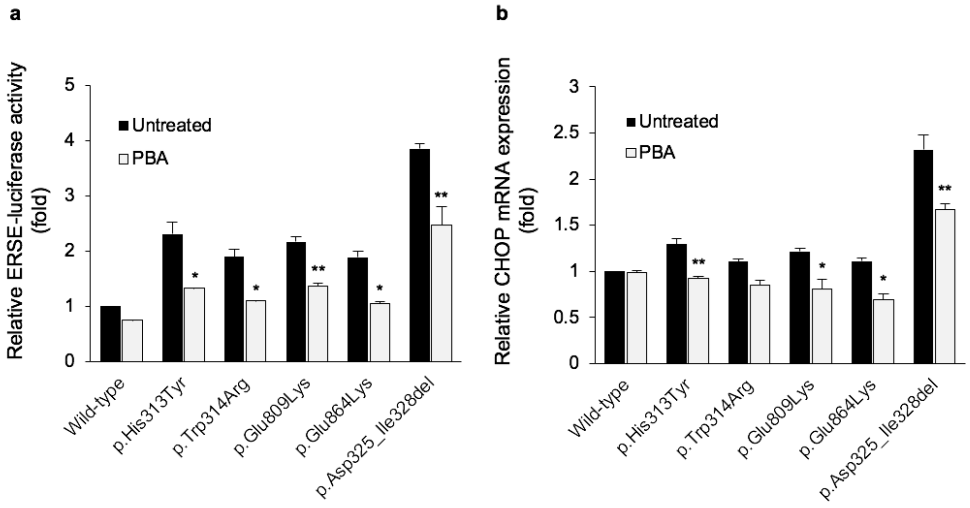

Figure 13. Effect of PBA in HEK293. a, Analysis of ERSE luciferase activity. HEK-293 cells were transfected with the ERSE reporter vector together with the wild-type or each WFS1 pathogenic variant (p. His313Tyr, p.Trp314Arg, p.Asp325_Ile328del, p.Glu809Lys, and p.Glu864Lys) expression plasmid. Transfected HEK-293 cells were treated with 4 mM PBA for 24 h. ERSE activity was normalized to *Renilla reniformis* luciferase activity. **b,** Quantitative PCR analysis of CHOP mRNA. After 4 h transfection, cells were treated with 0.5 mM PBA for 16 h. mRNA was extracted from the cells and RT-PCR was performed followed by quantitative PCR. CHOP mRNA levels were normalized by GAPDH. Values are represented as the mean ± SD. Statistical analysis was performed between groups untreated or treated by PBA using two tailed Student's *t*-test. Significant differences are indicated with $*p < 0.05$; $**p < 0.01$.

3.7. Effect of VPA

We also examined the effect of VPA on ERSE-luciferase activity and the expression level of CHOP mRNA. ER stress and the expression levels of CHOP mRNA of p.His313Tyr, p.Asp325_Ile328del, and p.Glu809Lys were also significantly reduced by VPA in MIN6 cells (Figure 14a, b). VPA reduced ERSE activity for each dominant variant n HEK-293 cells (Fig. 15a). For p.Asp325_Ile328del, p.Glu809Lys, and p.Glu864Lys, VPA treatment significantly reduced CHOP mRNA levels compared with wild-type WFS1. For p.His313Tyr and p.Trp314Arg, VPA treatment tended to reduce the expression of CHOP mRNA compared with wild-type WFS1 (Figure 15b).

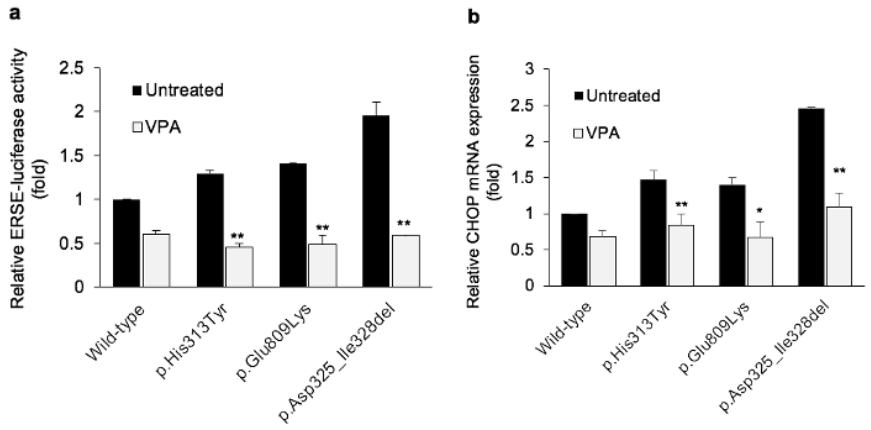

Figure 14. Effect of VPA in MIN6 cells. a, Analysis of ERSE luciferase activity. MIN6 cells were transfected with the ERSE reporter vector together with the wild-type or WFS1 variant (p. His313Tyr, p. Glu809Lys and p.Asp325_Ile328del) expression plasmid. Transfected MIN6 cells were treated with 6 mM VPA for 24 h. ERSE activity was normalized to *Renilla reniformis* luciferase activity. **b,** Quantitative PCR analysis of CHOP mRNA. After 4 h transfection, MIN6 cells were treated with 0.25 mM PBA for 16 h. mRNA was extracted from the cells and RT-PCR was performed followed by quantitative PCR. CHOP mRNA levels were normalized by GAPDH. Significant differences are indicated with $*p < 0.05$; $**p < 0.01$.

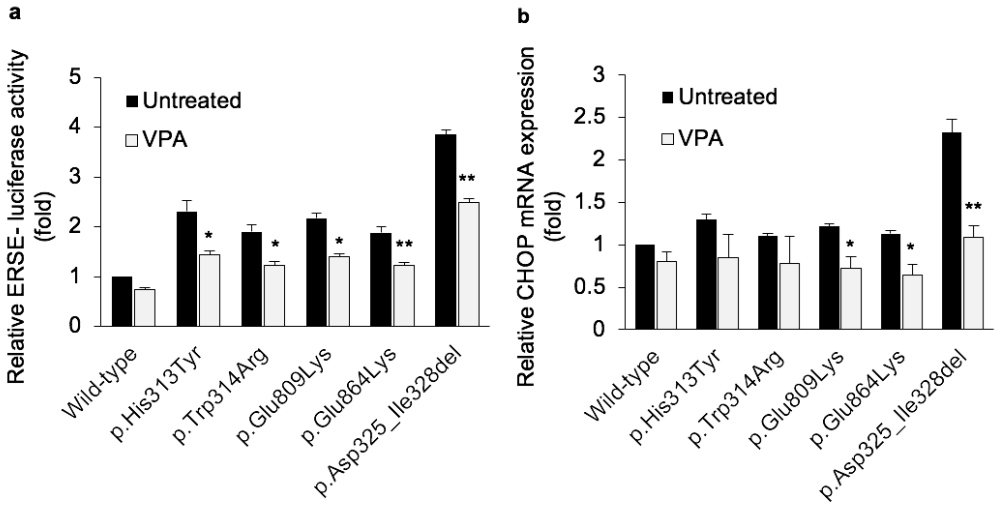

Figure 15. Effect of VPA in HEK-293 cells. a, Analysis of ERSE luciferase activity. Transfected HEK-293 cells were treated with 6 mM VPA for 24 h. ERSE activity was normalized by *Renilla reniformis* luciferase activity. **b,** Quantitative PCR analysis of CHOP mRNA. HEK-293 cells were transfected with the wild-type or each WFS1 variant (p.His313Tyr, p.Trp314Arg, p.Asp325_Ile328del, p.Glu809Lys, and p.Glu864Lys) expression plasmid. After 4 h transfection, cells were treated with 0.25 mM VPA for 16 h. mRNA was extracted from the cells and RT-PCR was performed followed by quantitative PCR. CHOP mRNA levels were normalized by GAPDH. Significant differences are indicated with $*p < 0.05$; $**p < 0.01$.

3.8 Effect of PBA and VPA on the localization of WFS1 pathogenic variants

Furthermore, we studied the effect of PBA and VPA on the localization of dominant WFS1 variants. Aggregations of each variant in the ER seemed to decrease, but there was no significant difference in the number of aggregates after PBA and VPA treatment (Figure 16).

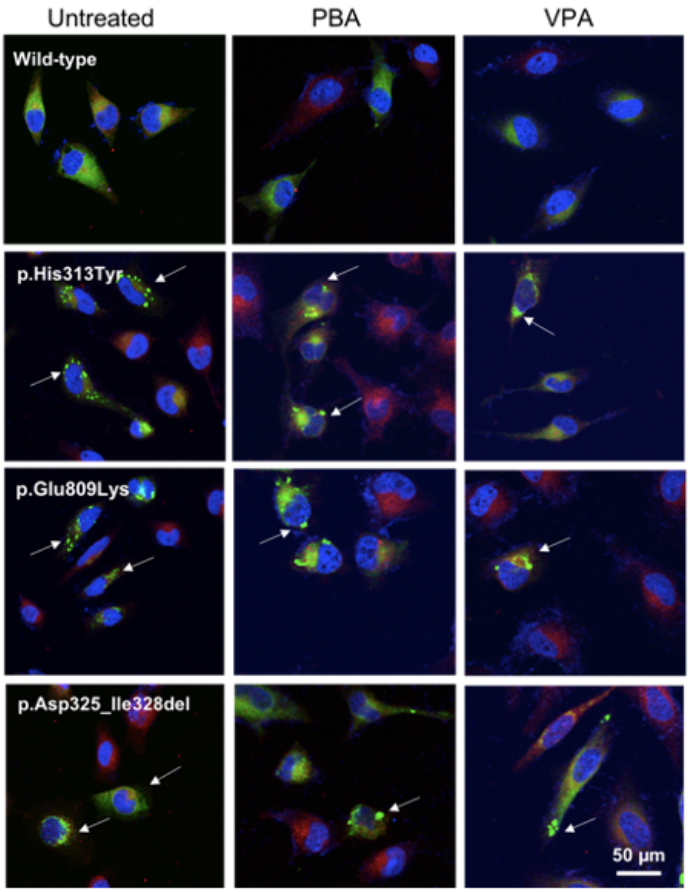

Figure 16. Effect of PBA and VPA on double immunofluorescence. HeLa cells were transiently transfected with the GFP-tagged wild-type or WFS1 variant (p.His313Tyr, p.Asp325_Ile328del, p.Glu809Lys) expression plasmid. At 24 h after transfection, cells were treated with or without 0.5mM PBA and 0.25 mM VPA for 16 hr. The location of the ER was detected using an ER-ID Red Assay Kit. The nuclei were stained blue (Hoechst 33342). Aggregations of each WFS1 variant (white arrows) in the ER tends to decrease. The aggregated cells were quantitatively analyzed using IN Cell Analyzer 1000, but there was no significant difference in the number of aggregates after PBA and VPA treatment (data not shown). ER was detected using an ER-ID Red Assay Kit, the nuclei were stained blue (Hoechst 33342). Scale bar 50μm. Each image was taken using a confocal microscopy.

4. Discussion

WS is usually inherited in an autosomal recessive manner and many of the reported recessive variants are dispersed throughout all of the domains of WFS1. In contrast, six dominant variants of WS have been reported to date [1,25-28]. It is of note that all of the dominant variants located in the first transmembrane domain (p.His313Tyr, p.Trp314Arg, and p.Asp325_Ile328del) are closely clustered (Figure 4). The dominant variants located in the ER lumen domain [26] changes of glutamic acid, i.e., p.Glu809Lys, p.Glu830Ala [27], and p.Glu864Lys [27,29,30]. The close localization of the mutations in the first transmembrane domain and the specific amino acid changes in the ER lumen domain may be related to the formation of the dominant variants. p.Glu864Lys is found in patients with autosomal dominant optic atrophy and hearing impairment [27,29,30], although the functional consequence of this mutation has not been determined. However, in the present report, we found that this variant elevated ER stress, similar to the other dominant variants in WFS1 [1,25,26]. Moreover, each dominant WFS1 variant demonstrated exerted dominant negative effect similar to previous studies of p.His313Tyr and p.Asp325_Ile328del [1,26]. Because WFS1 could forms multimer, which composed of dominant WFS1 variant and wild-type monomers are not structurally competent or fully functional, these variants exert the dominant negative effects. Our study has also shown that ATF6α promoter activity was activated in dominant WFS1 variants. The mechanism for this is speculated as follows. WFS1 recruits ATF6α to the E3 ligase HRD1 for ATF6 ubiquitination and proteasomal degradation [33]. While under conditions of ER stress, ATF6α disassociates from WFS1 and undergoes proteolysis, and the active form of ATF6α moves to the nucleus, leading to the regulation of the ER stress target genes CHOP, BIP, and XBP-1 [33]. Therefore, it is thought that the interaction between ATF6α and the dominant variants may be impaired, resulting in increased ER stress. This may be one of several mechanisms of increased ER stress by dominant WFS1 variants.

Because CHOP is involved in ER stress-induced apoptosis, we analyzed CHOP mRNA

levels using HEK-293 after transfection with each variant. As results, the expression levels of CHOP mRNA increased compared with wild-type WFS1, suggesting that the enhanced ER stress by these dominant variants led to cell apoptosis.

In addition, we performed same experiments with MIN6 cells for more physiological conditions. Similar to HEK-293 cells, ERSE and ATF6α promoter activity were activated by p.His313Tyr, p.Glu809Leu and p.Asp325_Ile328del. CHOP mRNA levels also increased in these variants. By contrast, luciferase activity of p.Trp314Arg and p.Glu864Lys did not increase compared to the wild-type. As WFS1 is highly expressed in MIN6 compared with HEK-293 cells, [65,66] MIN6 cells might be better reflected *in vivo.*

We tested whether recessive variants activate ERSE luciferase activity, ATF6α promoter activity and exert a dominant negative effect. By contrast recessive variants did not increase ER stress significantly and did not have a dominant negative effect in agreement with previous studies [26,67]. Based on these results, ER stress may be able to be caused by dominant variants themselves, rather than the effect of overexpression.

Regarding the effect of PBA and VPA, these agents alleviated ER stress and cell apoptosis caused by dominant variants. Indeed, all dominant variants localized to the ER as punctate granules of misfolded protein; thus, PBA may improve the accumulation of misfolded WFS1, thereby reducing ER stress. We studied the effect of PBA and VPA on the localization of dominant WFS1 variants. Aggregations of WFS1 variants were likely to reduce after the treatment of PBA and VPA, but we could not make a quantitative difference. Treatment of PBA and VPA might change protein folding of WFS1 variants, but our method was not sensitive to quantify the difference.

There are some limitations of our study. We did not perform the experiment from tissues from the patients with WFS1. In addition, the concentration of PBA and VPA in the experiment was a pharmacological concentration and it is difficult to increase it *in vitro*.

Furthermore, the effect of PBA and VPA in *in vivo* condition such as *Wfs1* knockout mice has not been studied. Therefore, further studies would be necessary to better understand the molecular mechanism of WFS1 and improve both prevention strategies and target treatments for this devastating disease.

Our present study demonstrated the dominant negative effect of each dominant WFS1 pathogenic variant. Moreover, PBA and VPA could reduce the ER stress and cell apoptosis caused by dominant WFS1 variants *in vitro.* Thus, these molecules may be effective to regulate ER stress-related cell apoptosis and could be used to delay the progression of WS and WS-like disorders caused by dominant WFS1 variants and other diseases associated with ER dysfunction.

5.Potential treatment approach and future perspectives for Wolfram syndrome

Chemical chaperones such as PBA and tauroursodeoxycholic acid are able to reverse ER stress-mediated β-cell death and neurodegeneration in WS patients by rescuing or stabilizing the native conformation of pathological variants of WFS1 proteins [36]. iPSCs induced by WFS1 are a good experimental model to evaluate the efficiency of these chemical chaperones [36]. Recent studies have also shown that drug repurposing may be useful for treatment of WS. Candidate drugs are ER stress modulators and substances that control ER calcium [68]. Lu et al. reported that ER calcium stabilizers such as dantrolene sodium can suppress cell death and dysfunction in neuronal and β-cells in *Wfs1* knockout mice, and in iPSC models of this disease [67]. This medicine has been approved for malignant hyperthermia and muscle spasm [67]. In addition, glucagon-like peptide (GLP)-1 receptor agonists can suppress β-cell apoptosis in cell models of WS [67] and can improve diabetes in *Wfs1* knockout mice [69].

It has been reported that administration of VPA to *Wfs1* knockout mice increased WFS1 expression in β-cells and improved DM [62,63].

Modulation of calcium homeostasis of β-cells is another target, because dysregulation of cytosolic calcium regulation and signaling has been identified in β-cells of WS [70]. Recently, calpain inhibitor XI has been effective for the normalization of cytosolic calcium and insulin secretion in rat insulinoma cells lacking WFS1 [70].

Finally, iPSCs from skin cells of patients could be edited and differentiated into insulin-producing β-cells [71]. The development of such regenerative medicine is also expected.

References

1. Morikawa S, Tajima T, Nakamura A, Ishizu K, Ariga T . A novel heterozygous mutation of the WFS1 gene leading to constitutive endoplasmic reticulum stress is the cause of Wolfram syndrome. *Pediatr Diabetes* 18:934-941, 2017
2. Rigoli L, Bramanti P, Di Bella C, De Luca F. Genetic and clinical aspects of Wolfram syndrome 1, a severe neurodegenerative disease. *Pediatr Research* 83:921, 2018
3. Urano F. Wolfram Syndrome: Diagnosis, Management, and Treatment. *Curr Diab Rep* 16:6-6, 2016
4. Global burden of diabetes. International Diabetes federation. *Diabetic atlas fifth edition*, 2011
5. Unger RH, Orci L Paracrinology of islets and the paracrinopathy of diabetes. *PNAS* 107:16009-16012, 2010
6. American Diabetes Association. Diagnosis and classification of diabetes mellitus. *Diabetes care* 33 Suppl 1:S62-S69, 2010
7. Clark AL, Urano F. Endoplasmic reticulum stress in beta cells and autoimmune diabetes. *Curr Opin Immunol* 43:60-66, 2016
8. Inzucchi SE, Bergenstal RM, Buse JB, Diamant M, Ferrannini E, Nauck M, Peters AL, Tsapas A, Wender R, Matthews DR, American Diabetes A, European Association for the Study of D:Management of hyperglycemia in type 2 diabetes: a patient-centered approach: position statement of the American Diabetes Association (ADA) and the European Association for the Study of Diabetes (EASD). *Diabetes care* 35:1364-1379, 2012
9. Della MT, Setian N, Savoldelli RD, Guedes DR, Kuperman H, Menezes Filho HC, Steinmetz L, Cominato L, Dichtchekenian V, Damiani D. Diabetes mellitus in childhood: an emerging condition in the 21st century. *Rev Assoc Med Bras* 62:594-601, 2016
10. Nadella S, Indyk JA, Kamboj MK. Management of diabetes mellitus in children and adolescents: engaging in physical activity. *Transl Pediatr* 6:215-224, 2017

11. Fendler W, Borowiec M, Baranowska-Jazwiecka A, Szadkowska A, Skala-Zamorowska E, Deja G, Jarosz-Chobot P, Techmanska I, Bautembach-Minkowska J, Mysliwiec M, Zmyslowska A, Pietrzak I, Malecki MT, Mlynarski W. Prevalence of monogenic diabetes amongst Polish children after a nationwide genetic screening campaign. *Diabetologia* 55:2631-2635, 2012

12. Irgens HU, Molnes J, Johansson BB, Ringdal M, Skrivarhaug T, Undlien DE, Søvik O, Joner G, Molven A, Njølstad PR 2. Prevalence of monogenic diabetes in the population-based Norwegian Childhood Diabetes Registry. *Diabetologia* 56:1512-1519, 2013

13. Johansson BB, Irgens HU, Molnes J, Sztromwasser P, Aukrust I, Juliusson PB, Søvik O, Levy S, Skrivarhaug T, Joner G, Molven A, Johansson S, Njølstad PR. Targeted next-generation sequencing reveals MODY in up to 6.5% of antibody-negative diabetes cases listed in the Norwegian Childhood Diabetes Registry. *Diabetologia* 60:625-635, 2017

14. Pihoker C, Gilliam LK, Ellard S, Dabelea D, Davis C, Dolan LM, Greenbaum CJ, Imperatore G, Lawrence JM, Marcovina SM, Mayer-Davis E, Rodriguez BL, Steck AK, Williams DE, Hattersley AT. Prevalence, characteristics and clinical diagnosis of maturity onset diabetes of the young due to mutations in HNF1A, HNF4A, and glucokinase: results from the SEARCH for Diabetes in Youth. *J Clin Endocrinol Metab* 98:4055-4062, 2013

15. Rubio-Cabezas O, Hattersley AT, Njølstad PR, Mlynarski W, Ellard S, White N, Chi DV, Craig ME. ISPAD Clinical Practice Consensus Guidelines 2014. The diagnosis and management of monogenic diabetes in children and adolescents. *Pediatr Diabetes* 15 Suppl 20:47-64, 2014

16. Shepherd M, Shields B, Hammersley S, Hudson M, McDonald TJ, Colclough K, Oram RA, Knight B, Hyde C, Cox J, Mallam K, Moudiotis C, Smith R, Fraser B, Robertson S, Greene S, Ellard S, Pearson ER, Hattersley AT. Systematic Population Screening, Using Biomarkers and Genetic Testing, Identifies 2.5% of the U.K. Pediatric Diabetes Population With Monogenic Diabetes. *Diabetes Care* 39:1879-1888, 2016

17. Schwitzgebel VM. Many faces of monogenic diabetes. J Diabetes Investig 5:121-133, 2014

18. Rubio-Cabezas O, Ellard S. Diabetes mellitus in neonates and infants: genetic heterogeneity, clinical approach to diagnosis, and therapeutic options. *Horm Res Paediatr* 80:137-146, 2013

19. Stanik J, Dusatkova P, Cinek O, Valentinova L, Huckova M, Skopkova M, Dusatkova L, Stanikova D, Pura M, Klimes I, Lebl J, Gasperikova D, Pruhova S. De novo mutations of GCK, HNF1A and HNF4A may be more frequent in MODY than previously assumed. *Diabetologia* 57:480-484, 2014

20. Hofmann S, Philbrook C, Gerbitz K-D, Bauer MF. Wolfram syndrome: structural and functional analyses of mutant and wild-type wolframin, the WFS1 gene product. *Hum Mol Genet* 12:2003-2012, 2003

21. Rigoli L, Lombardo F, Di Bella C. Wolfram syndrome and WFS1 gene. *Clin Genet* 79:103-117, 2011

22. Matsunaga K, Tanabe K, Inoue H, Okuya S, Ohta Y, Akiyama M, Taguchi A, Kora Y, Okayama N, Yamada Y, Wada Y, Amemiya S, Sugihara S, Nakao Y, Oka Y, Tanizawa Y. Wolfram syndrome in the Japanese population; molecular analysis of WFS1 gene and characterization of clinical features. *PloS one* 9:e106906-e106906, 2014

23. Barrett TG, Bundey SE, Macleod AF. Neurodegeneration and diabetes: UK nationwide study of Wolfram (DIDMOAD) syndrome. *Lancet* 346:1458-1463, 1995

24. Fraser FC, Gunn T. Diabetes mellitus, diabetes insipidus, and optic atrophy. An autosomal recessive syndrome? *J Med Genet* 14:190-193, 1977

25. Bonnycastle LL, Chines PS, Hara T, Huyghe JR, Swift AJ, Heikinheimo P, Mahadevan J, Peltonen S, Huopio H, Nuutila P, Narisu N, Goldfeder RL, Stitzel ML, Lu S, Boehnke M, Urano F, Collins FS, Laakso M. Autosomal dominant diabetes arising from a Wolfram syndrome 1 mutation. *Diabetes* 62:3943-3950, 2013

26. De Franco E, Flanagan SE, Yagi T, Abreu D, Mahadevan J, Johnson MB, Jones G, Acosta F, Mulaudzi M, Lek N, Oh V, Petz O, Caswell R, Ellard S, Urano F, Hattersley AT. Dominant ER Stress-Inducing WFS1 Mutations Underlie a Genetic Syndrome of Neonatal/Infancy-Onset

Diabetes, Congenital Sensorineural Deafness, and Congenital Cataracts. *Diabetes* 66:2044-2053, 2017

27. Eiberg H, Hansen L, Kjer B, Hansen T, Pedersen O, Bille M, Rosenberg T, Tranebjaerg L. Autosomal dominant optic atrophy associated with hearing impairment and impaired glucose regulation caused by a missense mutation in the WFS1 gene. *J Med Genet* 43:435-440, 2006

28. Hansen L, Eiberg H, Barrett T, Bek T, Kjærsgaard P, Tranebjærg L, Rosenberg T. Mutation analysis of the WFS1 gene in seven Danish Wolfram syndrome families; four new mutations identified. *Eur J Hum Genet* 13:1275-1284, 2005

29. Cryns K, Thys S, Van Laer L, Oka Y, Pfister M, Van Nassauw L, Smith RJH, Timmermans J-P, Van Camp G. The WFS1 gene, responsible for low frequency sensorineural hearing loss and Wolfram syndrome, is expressed in a variety of inner ear cells. *Histochem Cell Biol* 119:247-256, 2003

30. Fukuoka H, Kanda Y, Ohta S, Usami S-i. Mutations in the WFS1 gene are a frequent cause of autosomal dominant nonsyndromic low-frequency hearing loss in Japanese. *J Hum Genet* 52:510, 2007

31. Valéro R, Bannwarth S, Roman S, Paquis-Flucklinger V, Vialettes B. Autosomal dominant transmission of diabetes and congenital hearing impairment secondary to a missense mutation in the WFS1 gene. *Diabet Med* 25:657-661, 2008

32. Pallotta MT, Tascini G, Crispoldi R, Orabona C, Mondanelli G, Grohmann U, Esposito S. Wolfram syndrome, a rare neurodegenerative disease: from pathogenesis to future treatment perspectives. *J Transl Med* 17:238-238, 2019

33. Fonseca SG, Ishigaki S, Oslowski CM, Lu S, Lipson KL, Ghosh R, Hayashi E, Ishihara H, Oka Y, Permutt MA, Urano F. Wolfram syndrome 1 gene negatively regulates ER stress signaling in rodent and human cells. *J Clin Inverst* 120:744-755, 2010

34. Hara T, Mahadevan J, Kanekura K, Hara M, Lu S, Urano F. Calcium efflux from the endoplasmic reticulum leads to β-cell death. *Endocrinology* 155:758-768, 2014

35. Abreu D, Urano F. Current Landscape of Treatments for Wolfram Syndrome. *Trends Pharmacol Sci* 40:711-714, 2019

36. Shang L, Hua H, Foo K, Martinez H, Watanabe K, Zimmer M, Kahler DJ, Freeby M, Chung W, LeDuc C, Goland R, Leibel RL, Egli D. β-cell dysfunction due to increased ER stress in a stem cell model of Wolfram syndrome. *Diabetes* 63:923-933, 2014

37. Cagalinec M, Liiv M, Hodurova Z, Hickey MA, Vaarmann A, Mandel M, Zeb A, Choubey V, Kuum M, Safiulina D, Vasar E, Veksler V, Kaasik A. Role of Mitochondrial Dynamics in Neuronal Development: Mechanism for Wolfram Syndrome. *PLoS Biol* 14:e1002511, 2016

38. Chaussenot A, Bannwarth S, Rouzier C, Vialettes B, Mkadem SAE, Chabrol B, Cano A, Labauge P, Paquis-Flucklinger V. Neurologic features and genotype-phenotype correlation in Wolfram syndrome. *Ann Neurol* 69:501-508, 2011

39. Braakman I, Hebert DN. Protein folding in the endoplasmic reticulum. *Cold Spring Harb Perspect Biol* 5:a013201, 2013

40. Fonseca SG, Burcin M, Gromada J, Urano F. Endoplasmic reticulum stress in beta-cells and development of diabetes. *Curr Opin Pharmacol* 9:763-770, 2009

41. Fonseca SG, Fukuma M, Lipson KL, Nguyen LX, Allen JR, Oka Y, Urano F. WFS1 Is a Novel Component of the Unfolded Protein Response and Maintains Homeostasis of the Endoplasmic Reticulum in Pancreatic β-Cells. *J Biol Chem* 280:39609-39615, 2005

42. Lin T, Lee JE, Kang JW, Shin HY, Lee JB, Jin DI. Endoplasmic Reticulum (ER) Stress and Unfolded Protein Response (UPR) in Mammalian Oocyte Maturation and Preimplantation Embryo Development. *Int J Mol Sci* 20, 2019

43. Hetz C. The unfolded protein response: controlling cell fate decisions under ER stress and beyond. *Nat Rev Mol* 13:89-102, 2012

44. Hetz C, Zhang K, Kaufman RJ. Mechanisms, regulation and functions of the unfolded protein response. *Nat Rev Mol* 21:421-438, 2020

45. Scheuner D, Kaufman RJ. The Unfolded Protein Response: A Pathway That Links Insulin

Demand with β-Cell Failure and Diabetes. *Endocr Rev* 29:317-333, 2008

46. Oyadomari S, Takeda K, Takiguchi M, Gotoh T, Matsumoto M, Wada I, Akira S, Araki E, Mori M. Nitric oxide-induced apoptosis in pancreatic β cells is mediated by the endoplasmic reticulum stress pathway. *PNAS* 98:10845, 2001

47. Ozcan U, Cao Q, Yilmaz E, Lee AH, Iwakoshi NN, Ozdelen E, Tuncman G, Görgün C, Glimcher LH, Hotamisligil GS. Endoplasmic reticulum stress links obesity, insulin action, and type 2 diabetes. *Science* 306:457-461, 2004

48. Yusta B, Baggio LL, Estall JL, Koehler JA, Holland DP, Li H, Pipeleers D, Ling Z, Drucker DJ. GLP-1 receptor activation improves beta cell function and survival following induction of endoplasmic reticulum stress. *Cell Metab* 4:391-406, 2006

49. Laybutt DR, Preston AM, Akerfeldt MC, Kench JG, Busch AK, Biankin AV, Biden TJ. Endoplasmic reticulum stress contributes to beta cell apoptosis in type 2 diabetes. *Diabetologia* 50:752-763, 2007

50. Ishihara H, Takeda S, Tamura A, Takahashi R, Yamaguchi S, Takei D, Yamada T, Inoue H, Soga H, Katagiri H, Tanizawa Y, Oka Y. Disruption of the WFS1 gene in mice causes progressive beta-cell loss and impaired stimulus-secretion coupling in insulin secretion. *Hum Mol Genet* 13:1159-1170, 2004

51. Riggs AC, Bernal-Mizrachi E, Ohsugi M, Wasson J, Fatrai S, Welling C, Murray J, Schmidt RE, Herrera PL, Permutt MA. Mice conditionally lacking the Wolfram gene in pancreatic islet beta cells exhibit diabetes as a result of enhanced endoplasmic reticulum stress and apoptosis. *Diabetologia* 48:2313-2321, 2005

52. Delépine M, Nicolino M, Barrett T, Golamaully M, Lathrop GM, Julier C. EIF2AK3, encoding translation initiation factor 2-alpha kinase 3, is mutated in patients with Wolcott-Rallison syndrome. *Nat Genet* 25:406-409, 2000

53. Kolb PS, Ayaub EA, Zhou W, Yum V, Dickhout JG, Ask K. The therapeutic effects of 4-phenylbutyric acid in maintaining proteostasis. *Int J Biochem Cell Biol* 61:45-52, 2015

54. Yam GH-F, Gaplovska-Kysela K, Zuber C, Roth Jr. Sodium 4-Phenylbutyrate Acts as a Chemical Chaperone on Misfolded Myocilin to Rescue Cells from Endoplasmic Reticulum Stress and Apoptosis. *Invest Opthtalmo Vis Sci* 48:1683-1690, 2007

55. Zeitlin PL, Diener-West M, Rubenstein RC, Boyle MP, Lee CKK, Brass-Ernst L. Evidence of CFTR Function in Cystic Fibrosis after Systemic Administration of 4-Phenylbutyrate. *Mol Ther* 6:119-126, 2002

56. Huang A, Young TL, Dang VT, Shi Y, McAlpine CS, Werstuck GH. 4-phenylbutyrate and valproate treatment attenuates the progression of atherosclerosis and stabilizes existing plaques. *Atherosclerosis* 266:103-112, 2017

57. Kim D-S, Li B, Rhew KY, Oh H-W, Lim H-D, Lee W, Chae H-J, Kim H-R. The regulatory mechanism of 4-phenylbutyric acid against ER stress-induced autophagy in human gingival fibroblasts. *Arch Pharmacal Res* 35:1269-1278, 2012

58. Cadavez L, Montane J, Alcarraz-Vizán G, Visa M, Vidal-Fàbrega L, Servitja J-M, Novials A. Chaperones ameliorate beta cell dysfunction associated with human islet amyloid polypeptide overexpression. *PloS ONE* 9:e101797-e101797, 2014

59. Kakiuchi C, Ishigaki S, Oslowski CM, Fonseca SG, Kato T, Urano F. Valproate, a Mood Stabilizer, Induces WFS1 Expression and Modulates Its Interaction with ER Stress Protein GRP94. *PLoS ONE* 4:e4134, 2009

60. Kim AJ, Shi Y, Austin RC, Werstuck GH. Valproate protects cells from ER stress-induced lipid accumulation and apoptosis by inhibiting glycogen synthase kinase-3. *J Cell Sci* 118:89-99, 2005

61. Li Z, Wu F, Zhang X, Chai Y, Chen D, Yang Y, Xu K, Yin J, Li R, Shi H, Wang Z, Li X, Xiao J, Zhang H. Valproate Attenuates Endoplasmic Reticulum Stress-Induced Apoptosis in SH-SY5Y Cells via the AKT/GSK3β Signaling Pathway. *Int J Mol Sci* 18:315, 2017

62. Huang S, Zhu M, Wu W, Rashid A, Liang Y, Hou L, Ning Q, Luo X. Valproate pretreatment protects pancreatic β-cells from palmitate-induced ER stress and apoptosis by inhibiting

glycogen synthase kinase-3β. *J Biomed Sci* 21:38-38, 2014

63. Terasmaa A, Soomets U, Oflijan J. Wfs1 mutation makes mice sensitive to insulin-like effect of acute valproic acid and resistant to streptozocin. *J Physiol Biochem* 67, 2011

64. Yagi Y, Fushida S, Harada S, Kinoshita J, Makino I, Oyama K, Tajima H, Fujita H, Takamura H, Ninomiya I, Fujimura T, Ohta T, Yashiro M, Hirakawa K. Effects of valproic acid on the cell cycle and apoptosis through acetylation of histone and tubulin in a scirrhous gastric cancer cell line. *J Exp Clin Cancer Res* : CR 29:149-149, 2010

65. Ueda K, Kawano J, Takeda K, Yujiri T, Tanabe K, Anno T, Akiyama M, Nozaki J, Yoshinaga T, Koizumi A, Shinoda K, Oka Y, Tanizawa Y. Endoplasmic reticulum stress induces Wfs1 gene expression in pancreatic β-cells via transcriptional activation. *Eur J Endocrinol* 153:167, 2005

66. Yamada T, Ishihara H, Tamura A, Takahashi R, Yamaguchi S, Takei D, Tokita A, Satake C, Tashiro F, Katagiri H, Aburatani H, Miyazaki J-i, Oka Y. WFS1-deficiency increases endoplasmic reticulum stress, impairs cell cycle progression and triggers the apoptotic pathway specifically in pancreatic β-cells. *Hum Mol Genet* 15:1600-1609, 2006

67. Lu S, Kanekura K, Hara T, Mahadevan J, Spears LD, Oslowski CM, Martinez R, Yamazaki-Inoue M, Toyoda M, Neilson A, Blanner P, Brown CM, Semenkovich CF, Marshall BA, Hershey T, Umezawa A, Greer PA, Urano F. A calcium-dependent protease as a potential therapeutic target for Wolfram syndrome. *PNAS* 111:E5292-E5301, 2014

68. Calamini B, Morimoto RI. Protein homeostasis as a therapeutic target for diseases of protein conformation. *Curr Top Med Chem* 12:2623-2640, 2012

69. Toots M, Seppa K, Jagomäe T, Koppel T, Pallase M, Heinla I, Terasmaa A, Plaas M, Vasar E. Preventive treatment with liraglutide protects against development of glucose intolerance in a rat model of Wolfram syndrome. *Sci Rep* 8:10183. 2018

70. Nguyen LD, Fischer TT, Abreu D, Arroyo A, Urano F, Ehrlich BE. Calpain inhibitor and ibudilast rescue β cell functions in a cellular model of Wolfram syndrome. *PNAS* 117:17389-17398, 2020

71. Maxwell KG, Augsornworawat P, Velazco-Cruz L, Kim MH, Asada R, Hogrebe NJ, Morikawa S, Urano F, Millman JR. Gene-edited human stem cell-derived β cells from a patient with monogenic diabetes reverse preexisting diabetes in mice. *Sci Transl Med*. 540:eaax9106, 2020